ticularly advantageous for in vivo studies in which the rapid activation of a gene is required, because, in contrast to the authentic tTA system, the kinetics of induction does not depend on the biological half-life of the effector.

REFERENCES AND NOTES

1. G. T. Yarronton, *Curr. Opin. Biotechnol.* **3**, 506 (1992).
2. M. Gossen, A. Bonin, H. Bujard, *Trends Biochem. Sci.* **18**, 471 (1993).
3. M. Gossen and H. Bujard, *Proc. Natl. Acad. Sci. U.S.A.* **89**, 5547 (1992).
4. W. Hillen and C. Berens, *Annu. Rev. Microbiol.* **48**, 345 (1994).
5. The mutagenesis and selection procedure was described previously [B. Hecht, G. Mller, W. Hillen, *J. Bacteriol.* **175**, 1206 (1993)].
6. W. Hinrichs *et al.*, *Science* **264**, 418 (1994).
7. G. Müller, thesis, Universität Erlangen-Nürnberg, Germany (1995).
8. To transfer the reverse DNA binding behavior of rTetR to tTA (*3*), a 399–base pair Xba I–Eco47 III fragment containing the relevant mutations of the *rtetR* gene was exchanged for the corresponding restriction fragment in pUHD15-1neo (an expression vector for tTA, consisting of a cytomegalovirus (CMV) promoter-enhancer, the gene encoding tTA, and an SV40 polyadenylation site) (*3*). In addition, the vector contains a pSV2neo-derived neomycin resistance cassette [P. J. Southern and P. Berg, *J. Mol. Appl. Genet.* **1**, 327 (1982)] to facilitate selection of transfected cells. Stable clones were selected at 500 μg of G418 per milliliter. The resulting expression vector for rtTA was named pUHD17-1neo.
9. A nuclear, localized tTA protein, tTA-nls, was constructed by fusion at the DNA level of a nuclear localization sequence to the NH_2-terminus of tTA. The functionality of the protein with respect to its transactivation capacity and enrichment in the nucleus was demonstrated [A. Kistner, thesis, University of Heidelberg, Germany (1993)]. The actual NH_2-terminal amino acid sequence of this protein is MPKRPRPS . . . (*16*); the underlined serine is amino acid residue 2 of tTA (*3*). The rtTA-nls expression vector pUHD172-1 is a derivative of pUHD152-1 that encodes tTA-nls.
10. M. Gossen, data not shown.
11. The luciferase reporter units used were pUHC13-3 (*3*) and pUHC13-7. In the latter, the CMV minimal promoter of pUHC13-3 is substituted by the HSV–thymidine kinase (TK) promoter truncated at position −37 relative to the transcriptional start site. The β-galactosidase reporter plasmid pUHG16-3 with a CMV minimal promoter has been described [D. Resnitzky, M. Gossen, H. Bujard, S. I. Reed, *Mol. Cell. Biol.* **14**, 1669 (1994)]. Transcription from these reporter units can be stimulated by both tTA and rtTA–rtTA-nls. The reporter plasmids were cotransfected with hygromycin selection markers. Selection was at 300 μg of hygromycin per milliliter.
12. Total RNA was prepared as described [P. Chomczynski and N. Sacchi, *Anal. Biochem.* **162**, 156 (1987)]. Northern (RNA) blot analysis was done according to standard procedures [J. Sambrook, E. F. Fritsch, T. Maniatis, *Molecular Cloning: A Laboratory Manual* (Cold Spring Harbor Laboratory, Cold Spring Harbor, NY, 1989)]. RNA was transferred onto NYTRAN membranes (Schleicher and Schüll, Dassel, Germany) and hybridized at 65°C [G. Church and W. Gilbert, *Proc. Natl. Acad. Sci. U.S.A.* **81**, 1991 (1984)] with probes prepared by the random primer technique [A. Feinberg and B. Vogelstein, *Anal. Biochem.* **132**, 6 (1983)]. The highest stringency wash was 0.2× sodium chloride sodium citrate buffer (SSC)/0.2% SDS. For quantitation, DNA probes of the *lacZ* gene and a GAPDH complementary DNA were simultaneously hybridized.
13. P. Weinmann, M. Gossen, W. Hillen, H. Bujard, C. Gatz, *Plant J.* **5**, 559 (1994).
14. P. A. Furth *et al.*, *Proc. Natl. Acad. Sci. U.S.A.* **91**, 9302 (1994).
15. Mice doubly transgenic for the luciferase reporter unit (*11*) and for tTA controlled by the CMV IE promoter (*3*) show high luciferase activity in organs where the CMV IE promoter is known to be active. Supply of doxycycline (200 μg/ml) in drinking water given to mice reduces the luciferase activity to background levels. Double-transgenic mice that express rtTA show the reverse phenotype. In both systems, regulatory factors of up to six orders of magnitude can be monitored, depending on the particular organ (A. Kistner and H. Bujard, in preparation).
16. Single-letter abbreviations for the amino acid residues are as follows: K, Lys; M, Met; P, Pro; R, Arg; and S, Ser.

17. We thank W. Hinrichs and W. Saenger for providing the coordinates to produce Fig. 2, S. Reinig for secreterial support in the preparation of the manuscript, and U. Baron for helpful suggestions. Supported by the Deutsche Forschungsgemeinschaft (SFB 229), by the Fonds der Chemischen Industrie Deutschlands, and by the E. C. BRIDGE RTD Programme.

19 December 1994; accepted 23 March 1995

Construction of a Soluble Adenylyl Cyclase Activated by $G_s\alpha$ and Forskolin

Wei-Jen Tang* and Alfred G. Gilman

A soluble adenylyl cyclase was constructed by linkage of portions of the cytosolic domains of the mammalian type I and type II enzymes. The soluble enzyme was stimulated by both forskolin and the α subunit of the heterotrimeric guanine nucleotide–binding protein (G protein) G_s ($G_s\alpha$). Expression of the construct complemented the catabolic defect in a strain of *Escherichia coli* that is deficient in adenylyl cyclase activity. The active, approximately 60-kilodalton enzyme accumulated in the cytoplasmic fraction of *E. coli* to yield activities in excess of 1 nanomole per minute per milligram of protein. The two sets of transmembrane helices of mammalian adenylyl cyclases are thus not necessary for the catalytic or the most characteristic regulatory activities of the enzyme. This system may be useful for both genetic and biochemical analysis of G protein–regulated adenylyl cyclases.

The structures of G protein–regulated adenylyl cyclases are complex, consisting of two intensely hydrophobic domains (M_1 and M_2), each hypothesized to contain six transmembrane helices, and two ~40-kD cytosolic domains (C_1 and C_2). The C_1 and C_2 domains contain sequences (C_{1a} and C_{2a}) that are similar to each other, to the corresponding regions of related adenylyl cyclases, and to the catalytic domains of membrane-bound and soluble guanylyl cyclases (*1*, *2*). Analysis of a series of truncation and alanine-scanning mutants of mammalian adenylyl cyclases indicates that both C_{1a} and C_{2a} (but not C_{1b} and C_{2b}) are necessary for catalytic activity (*3*, *4*). However, by analogy with the guanylyl cyclases, the hydrophobic domains are thought not to be so required. Membrane-bound adenylyl cyclases are expressed in small amounts, and the enzymes are labile and difficult to manipulate in detergent-containing solutions. We have thus attempted to construct a soluble adenylyl cyclase that retains regulatory properties of interest and that is amenable to both biochemical and genetic analysis.

Concurrent expression of the NH_2-terminal half of type I adenylyl cyclase and the COOH-terminal half of type II adenylyl cyclase results in the formation of a noncovalent chimera that remains sensitive to both $G_s\alpha$ and forskolin, despite extremely low basal activity (*4*). We have thus ligated complementary DNAs (cDNAs) that encode C_{1a} from type I adenylyl cyclase and C_{2a} from type II adenylyl cyclase with short linkers between them, resulting in constructs designated IC_1IIC_2-L_1, IC_1IIC_2-L_3, and IC_1IIC_2-L_5 (Fig. 1A) (*5*). To investigate whether these constructs encode functional adenylyl cyclases, we tested complementation of the catabolic defect in *E. coli* Δcya TP2000, which lacks adenylyl cyclase activity (*6*). This deficient bacterial strain cannot use maltose as a carbon source; colonies thus fail to turn red on McConkey agar and do not grow on minimal medium (*7*). To activate adenylyl cyclase in *E. coli*, we coexpressed the cyclase constructs with either wild-type $G_s\alpha$ or a mutant $G_s\alpha$ (in which Gln^{227} is replaced with Leu; designated $G_s\alpha$*) that is deficient in guanosine triphosphatase (GTPase) activity and is thus constitutively active (*8*). *Escherichia coli* TP2000 expressing either $G_s\alpha$ or $G_s\alpha$* remained pale yellow on McConkey agar supplemented with maltose and failed to grow on minimal medium (M63 medium containing arginine and maltose) (Fig. 1B). However, bacteria expressing $G_s\alpha$* and any of the three chimeric adenylyl cyclase constructs turned red on McConkey agar and grew on minimal medium (Fig. 1B). (Wild-

Department of Pharmacology, University of Texas Southwestern Medical Center, Dallas, TX 75235, USA.

*Present address: Department of Pharmacological and Physiological Sciences, University of Chicago, Chicago, IL 60637, USA.

type *E. coli* turn red in about half the time required for the chimeric constructs.) Correction of the catabolic defect was also evident when wild-type $G_s\alpha$ was expressed with IC_1IIC_2-L_3 or IC_1IIC_2-L_5, but longer times were required. There was evidence of a small amount of adenosine 3′,5′-monophosphate (cAMP) synthesis when construct IIC_2 was coexpressed with $G_s\alpha$*; no such effect was apparent with IC_1 (Fig. 1B). Similar ligation of C_{1a} and C_{2a} from type I adenylyl cyclase failed to produce a functional enzyme by these criteria (9).

We also tested four mutants of $G_s\alpha$ that are altered in positions corresponding to the α3-β5 and α4-β6 loops of $G_t\alpha$ and $G_{i1}\alpha$ and the α3 helix (*10*, *11*); these mutants have a reduced ability to activate adenylyl cyclase (*12*). The cDNAs encoding these proteins were also altered to substitute Cys for Arg^{201}, a mutation that also inhibits GTPase activity and activates the α subunit. We transferred these cDNAs into the expression vector and tested their ability to activate IC_1IIC_2-L_3 in *E. coli* (9). As a control, *E. coli* Δcya turned red on McConkey agar when transformed with vectors encoding $G_s\alpha(Arg^{201}\rightarrow Cys)$ and IC_1IIC_2-L_3. Under the same conditions, $G_s\alpha$ with a mutation in the α3 helix failed to show activity, whereas the other three mutants were indistinguishable from the control protein. These results correlate well with those obtained by transient expression of these proteins in HEK 293 cells.

We examined adenylyl cyclase activity in vitro in 150,000*g* supernatant fractions from *E. coli* TP2000 transformed with the various constructs (*13*). The soluble fraction from cells containing a control plasmid had no detectable adenylyl cyclase activity (Fig. 1C). In contrast, supernatants from cells expressing IC_1IIC_2-L_1, IC_1IIC_2-L_3, or IC_1IIC_2-L_5 showed basal adenylyl cyclase activity (~2 pmol/min per milligram of protein) that was activated by 200 nM $G_s\alpha$ bound to guanosine 5′-*O*-(3-thiotriphosphate) (GTP-γ-S) (50-fold), 100 μM forskolin (150- to 200-fold), or a combination of the two (600-fold). The combination of Ca^{2+} and calmodulin had no detectable effect on activity, and lysates from cells expressing either IC_1 or IIC_2 showed little adenylyl cyclase activity.

Although forskolin appeared not to activate adenylyl cyclase in vivo when present alone, a synergistic interaction between forskolin and wild-type $G_s\alpha$ was evident with constructs IC_1IIC_2-L_3 or IC_1IIC_2-L_5 (Fig. 1B). In view of the stimulatory effects of forskolin in vitro, these modest effects of the diterpene in vivo presumably result from its failure to reach sufficiently high intracellular concentrations. To test this hypothesis, we attempted to increase the accumulation of cAMP intracellularly by constructing a mutant deficient in cyclic nucleotide phosphodiesterase (cpd^-). An *E. coli* strain lacking both adenylyl cyclase and the phosphodiesterase grew on minimal medium containing one-tenth the concentration of cAMP required to allow growth of the corresponding strain that expressed cyclic nucleotide phosphodiesterase (9). We treated cells with polymyxin B nanopeptide, which integrates into the outer membrane of Gram-negative bacteria and forms a pore structure, thereby increasing their permeability to hydrophobic compounds by up to 300-fold (*14*). *Escherichia coli* Δcya, cpd^- did not grow on maltose minimal medium in the presence of forskolin (10 μM) and polymyx-

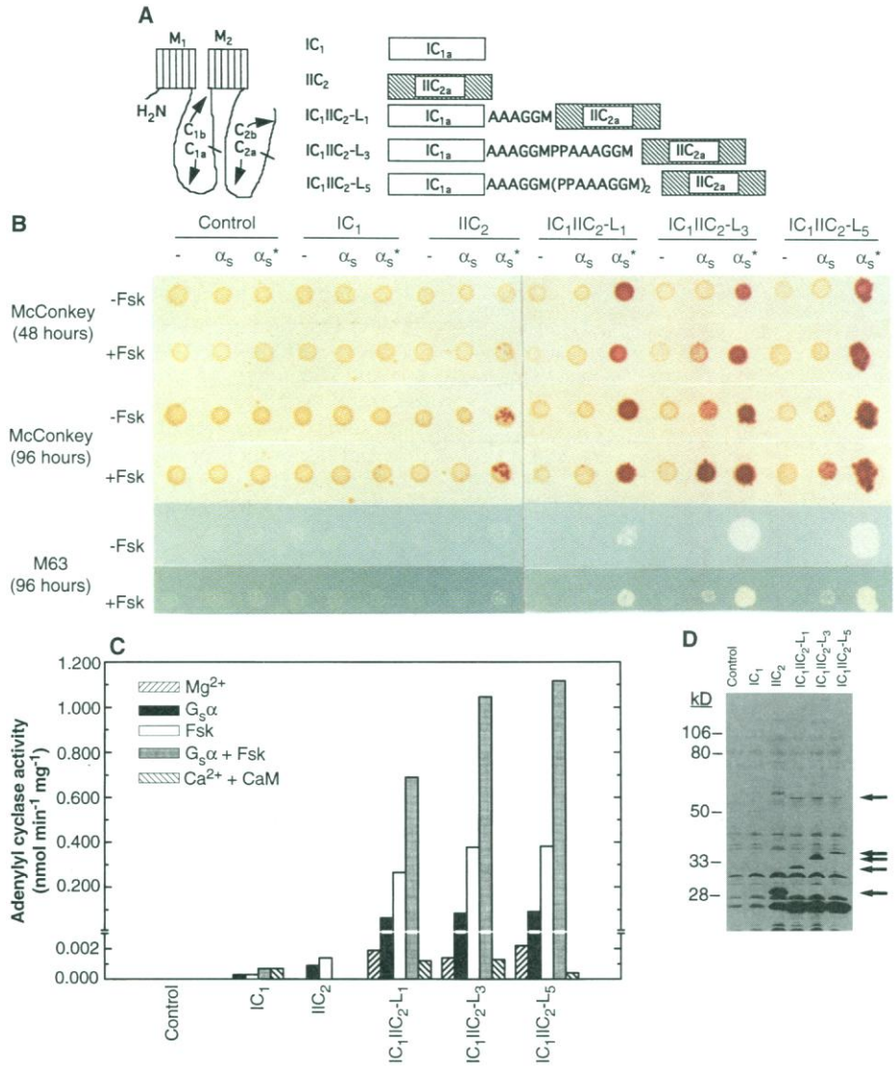

Fig. 1. Properties of soluble type I–type II adenylyl cyclase chimeras expressed in *E. coli*. (**A**) A model of mammalian adenylyl cyclase (left) and the various chimeras between type I and type II adenylyl cyclases (right); the linker sequences are also shown (A, Ala; G, Gly; M, Met; and P, Pro). IC_{1a} includes residues 271 to 484 of type I adenylyl cyclase; IIC_{2a} includes residues 821 to 1090 of type II adenylyl cyclase. No sequences from any of the putative transmembrane spans of either enzyme are included. (**B**) Phenotypic complementation. *Escherichia coli* TP2000 bacteria were transformed with two compatible plasmids, one for the expression of $G_s\alpha$ and the other for expression of the adenylyl cyclase constructs. Transformants were selected for resistance to carbenicillin and kanamycin, and bacteria were cultured on either McConkey or M63 agar containing 0.4% maltose, 50 μM carbenicillin, 50 μM kanamycin, and 100 μM isopropyl-β-D-thiogalactopyranoside. Cells were grown at 30°C for the indicated times. Forskolin (5 μl, 10 mM) was spotted on the plates where indicated (+Fsk) before addition of transformants. (**C**) Enzyme activity of the chimeras. Adenylyl cyclase activities of supernatant fractions of lysates (20 μg) from *E. coli* containing the indicated plasmids were assayed with 10 mM $MgCl_2$ at 30°C for 30 min. Assays also contained 200 nM GTP-γ-S–$G_s\alpha$ ($G_s\alpha$), 100 μM forskolin (Fsk), or 100 μM $CaCl_2$ plus 2 μM calmodulin (Ca^{2+} + CaM), as indicated. (**D**) Immunoblot analysis with antiserum C2-1077 of 150,000*g* supernatants from lysates of *E. coli* containing the indicated plasmids (*30*). Immunoreactive proteins of 60, 36, 34, 32, and 29 kD (arrows) as well as the positions of molecular size standards (left) are indicated. Data shown are representative of at least two experiments.

in B nanopeptide (33 μg/ml). However, the bacteria did grow under these conditions if they also expressed the adenylyl cyclase construct IC_1IIC_2-L_3. This observation supports the hypothesis that the ineffectiveness of forskolin in vivo results from its poor permeability through the outer membrane of *E. coli*.

The expected 60-kD protein was detected in appropriate *E. coli* supernatants with an antiserum to the COOH-terminus of type II adenylyl cyclase (antiserum C2-1077) (Fig. 1D), although the signal was not strong. The appropriate 29-kD soluble protein was present in cells expressing IIC_2. We also detected 32-, 34-, and 36-kD proteins in cells expressing IC_1IIC_2-L_1, IC_1IIC_2-L_3, or IC_1IIC_2-L_5, respectively. Other smaller proteins were present in extracts from all cells containing IIC_2 cDNA. These proteins may arise from proteolysis or initiation of translation from downstream sites.

Adenylyl cyclase activity in 150,000*g* supernatants from cells expressing IC_1IIC_2-L_3 was stimulated by addition of either forskolin (Fig. 2A) or GTP-γ-S–$G_s\alpha$ (Fig. 2B). The median effective concentration (EC_{50}) for forskolin was ~7 μM. A forskolin analog, 1,9-dideoxyforskolin, which does not activate mammalian adenylyl cyclases (*15*), also failed to stimulate this enzyme. The EC_{50} for activation of IC_1IIC_2-L_3 by GTP-γ-S–$G_s\alpha$ was ~1 μM, a value 20 to 50 times greater than that observed with type I or type II adenylyl cyclase. However, the maximal stimulatory effect of the G protein α subunit exceeded that of forskolin (Fig. 2B). The stimulatory effects of minimally effective concentrations of GTP-γ-S–$G_s\alpha$ and forskolin were synergistic (Fig. 2C), which is also characteristic of several mammalian adenylyl cyclases (*16*). When IC_1IIC_2-L_3 was activated with forskolin or GTP-γ-S–$G_s\alpha$, values of the Michaelis constant (K_m) for adenosine triphosphate (ATP) were 0.44 and 0.11 mM, respectively (Fig. 2D). Addition of GTP-γ-S–$G_s\alpha$ in the presence of forskolin did not change the K_m. Synergistic activation of the enzyme was thus not attributable to alteration of apparent substrate affinity.

Forskolin regulates the functions of several intrinsic membrane proteins, including adenylyl cyclases (*17*), glucose transporters (*18, 19*), voltage-gated K^+ channels (*20*), nicotinic cholinergic receptors (*21*), a γ-aminobutyric acid receptor (*22*), and P glycoproteins (*23, 24*). These proteins share no obvious amino acid sequence similarity. However, all have one or more hydrophobic domains predicted to include four or six transmembrane helices, and forskolin is highly lipophilic. Attempts to map forskolin binding sites have implicated the transmembrane helices or residues immediately adjacent to these domains (*25, 26*). We were thus surprised to detect activation of the IC_1IIC_2 constructs by forskolin. It is possible that the interaction of forskolin with adenylyl cyclase differs from that with other proteins. Although forskolin activates adenylyl cyclases, it inhibits or blocks the pore conductivity of the other forskolin-regulated proteins.

The G protein βγ subunit complex (to 1 μM) and myristoylated GTP-γ-S–$G_{i1}\alpha$ (2 μM) had little effect on the basal or stimulated activities of IC_1IIC_2-L_3 (9); $MnCl_2$ (5 mM) inhibited the activated enzyme (50 to 80%). Forskolin-activated IC_1IIC_2-L_3 was inhibited noncompetitively by 2′-deoxy-3′-AMP (a so-called P-site inhibitor) (Fig. 2E). The enzyme was most sensitive to inhibition by the P-site analog when it was maximally stimulated by both forskolin and GTP-γ-S–$G_s\alpha$. These properties are characteristic of P-site inhibition of mammalian adenylyl cyclases (*27, 28*).

A supernatant containing IC_1IIC_2-L_3

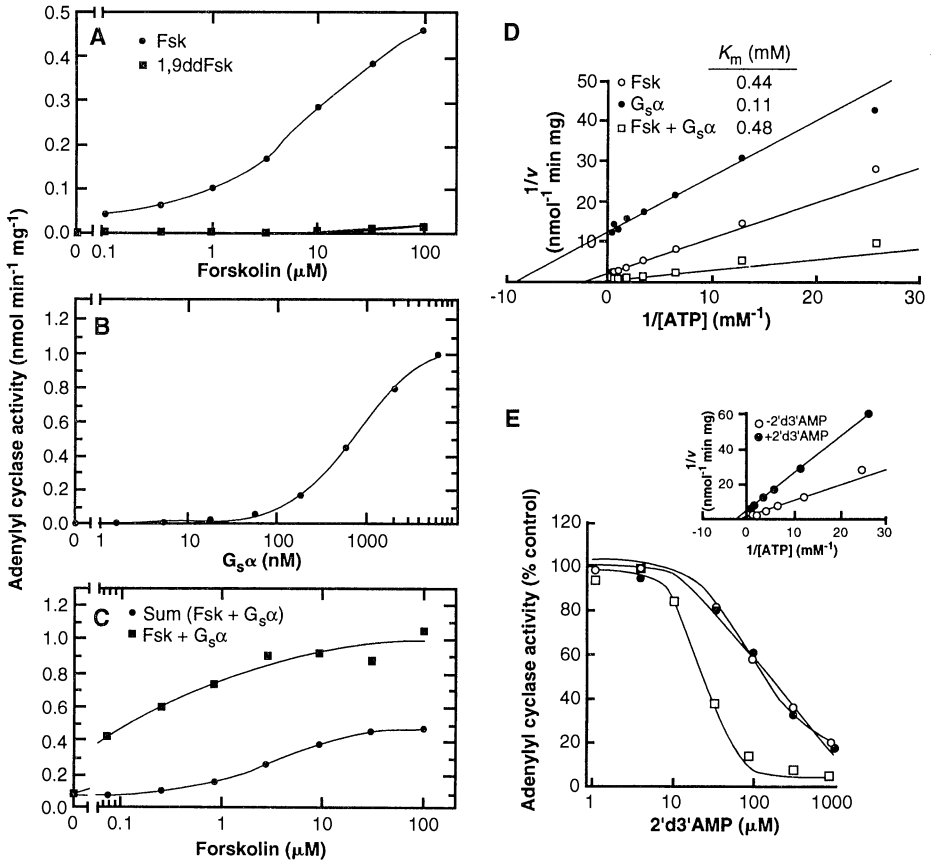

Fig. 2. Enzymatic activity of IC_1IIC_2-L_3. (**A**) Activation of soluble adenylyl cyclase by forskolin (Fsk), but not by 1,9-dideoxyforskolin (1,9-ddFsk). (**B**) Activation by GTP-γ-S–$G_s\alpha$. (**C**) Synergistic activation by GTP-γ-S–$G_s\alpha$ and forskolin. The concentration of GTP-γ-S–$G_s\alpha$ was 200 nM. Sum (Fsk + $G_s\alpha$) is the sum of adenylyl cyclase activities observed in the presence of forskolin or GTP-γ-S–$G_s\alpha$ alone; Fsk + $G_s\alpha$ is adenylyl cyclase activity observed in the presence of both GTP-γ-S–$G_s\alpha$ and forskolin. (**D**) Determination of K_m values for ATP. The concentrations of forskolin and GTP-γ-S–$G_s\alpha$ were 10 μM and 200 nM, respectively. (**E**) Effect of 2′-deoxy-3′-AMP (2′d3′AMP). The adenylyl cyclase activity of a supernatant fraction (20 μg) from *E. coli* expressing IC_1IIC_2-L_3 was assayed at 30°C for 30 min in the presence of 10 μM forskolin (○), 200 nM GTP-γ-S–$G_s\alpha$ (●), or forskolin plus GTP-γ-S–$G_s\alpha$ (□); control activities for these conditions were 270, 95, and 970 pmol/min per milligram of protein, respectively. (**Inset**) Activity was assayed in the presence of 10 μM forskolin. Data are representative of at least two experiments.

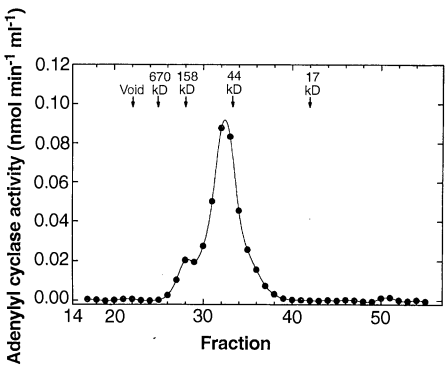

Fig. 3. Superdex 75 gel-filtration chromatography of an extract containing IC_1IIC_2-L_3 (*31*). Molecular size markers are thyroglobulin (670 kD), γ-globulin (158 kD), chicken ovalbumin (44 kD), and horse myoglobin (17 kD). Total activity was 1.02 nmol/min per milliliter and recovery was 71%. Data are representative of two experiments.

was subjected to gel filtration through Pharmacia Superdex 75; a major peak of adenylyl cyclase activity consistent with a globular 60-kD protein was observed, as well as a minor peak consistent with a protein of about twice the size (Fig. 3). The active enzyme thus appears to migrate as a monomer, although a small fraction may be present as dimers. The 60-kD immunoreactive band (Fig. 1D) was present within the major peak of adenylyl cyclase activity, whereas the 27- and 34-kD bands were not. Proteolysis was evident in these extracts; further chromatography of the material shown in Fig. 3 on a Pharmacia Mono Q column revealed multiple peaks of activity, and only a fraction of the active enzyme was recognized by antiserum C2-1077 (directed against the COOH-terminus). This expression system and the resulting protein should facilitate genetic, biochemical, and, perhaps, structural analysis of this complex group of enzymes (*29*).

REFERENCES AND NOTES

1. W.-J. Tang and A. G. Gilman, *Cell* **70**, 869 (1992).
2. R. Taussig and A. G. Gilman, *J. Biol. Chem.* **270**, 1 (1995).
3. W.-J. Tang, J. A. Iñiguez-Lluhi, S. M. Mumby, A. G. Gilman, *Cold Spring Harbor Lab. Symp. Quant. Biol.* **57**, 135 (1992).
4. W.-J. Tang, M. Stanzel, A. G. Gilman, in preparation.
5. To produce DNA for expression of IC_1, we introduced sites for restriction enzymes Nco I and Not I at nucleotide 704 (amino acid residue 237 of type I adenylyl cyclase) and nucleotide 1453 (amino acid residue 484 of type I adenylyl cyclase), respectively, and an internal Nco I site was eliminated by two rounds of mutagenesis with M13-mp18-C_1 as the template (*4*) [T. A. Kunkel, J. D. Roberts, R. A. Zabour, *Methods Enzymol.* **154**, 367 (1987)]. The 0.7-kb Nco I–Eco RI fragment was cloned into the same sites of the prokaryotic expression vector pTrcHisA (Invitrogen, San Diego, CA), resulting in pTrc-IsC_1. A termination site was introduced by adding phosphorylated linkers (5′-GGCCGCTCACCATCACCATCACCATTAGG and 5′-AATTCCTAATGGTGATGGTGATGGTGAGC) to pTrc-IsC_1 that had been digested with Not I and Eco RI; the resulting plasmid was used for expression of IC_1. To produce DNA for expression of IIC_2, we isolated a 0.9-kb Ssp I–Kpn I fragment from pSK-rACII [pBluescript (Stratagene) with a cDNA insert that encodes type II adenylyl cyclase]. This fragment was ligated with phosphorylated linkers (5′-GATCCATCATGAGACAGAGTGAAT and 5′-ATTCACTCTGTCTCATGATG) and pUC18 that had been digested with Bam HI and Kpn I, resulting in pUC-IIC_2. The 0.9-kb Bsp HI–Eco RI fragment from pUC-IIC_2 was transferred to pTrcHisA that had been digested with Nco I and Eco RI, for expression of IIC_2 (residues 821 to 1090 of type II adenylyl cyclase). To link IC_1 and IIC_2, we ligated the 0.9-kb Bsp HI–Eco RI fragment from pUC-IIC_2 with phosphorylated linkers (5′-GGCCGCTGGAGG and 5′-GATGCCTCCAGC) and pTrc-IsC_1 that had been digested with Not I and Eco RI. One, three, or five sets of linkers were incorporated, resulting in pTrc-IC_1IIC_2-L_1, pTrc-IC_1IIC_2-L_3, and pTrc-IC_1IIC_2-L_5, respectively. A small deletion (56 base pairs) at the sequence encoding the NH_2-terminus of IC_1IIC_2 (immediately after the Nco I site) occurred during subcloning. The site of initiation of IC_1IIC_2-L_3 is thus residue 271. To express $G_s\alpha$, we ligated a 1.3-kb Nco I (blunted)–Hind III fragment encoding either $G_s\alpha$-l or the Gln^{227}→Leu mutant of $G_s\alpha$-l with the 4.5-kb Nco I (blunted)–Eco RI fragment from pBB131 [L. J. Knoll and J. I. Gordon, *J. Biol. Chem.* **268**, 4281 (1993)].
6. A. Roy and A. Danchin, *Mol. Gen. Genet.* **188**, 465 (1982); A. Beuve, B. Boesten, M. Crasnier, A. Danchin, F. O'Gara, *J. Bacteriol.* **172**, 2614 (1990).
7. R. Perlman and I. Pastan, *Biochem. Biophys. Res. Commun.* **37**, 151 (1969).
8. M. P. Graziano and A. G. Gilman, *J. Biol. Chem.* **264**, 15475 (1989).
9. W.-J. Tang and A. G. Gilman, unpublished data.
10. J. P. Noel, H. E. Hamm, P. B. Sigler, *Nature* **366**, 654 (1993).
11. D. E. Coleman *et al.*, *Science* **265**, 1405 (1994).
12. C. H. Berlot and H. R. Bourne, *Cell* **68**, 911 (1992).
13. *Escherichia coli* bacteria that contained the desired plasmids were grown in LB medium containing 50 μM carbenicillin to an optical density at 600 nm of 0.3. Isopropyl-β-D-thiogalactopyranoside (100 μM) and chloramphenicol (0.5 μM) were added to the medium to induce expression of adenylyl cyclase for 12 hours. Bacteria were then collected by centrifugation at 4°C and lysed by incubation at 4°C for 30 min in 20 mM tris-HCl (pH 8.0), 1 mM EDTA, 2 mM dithiothreitol, protease inhibitors, and lysozyme (0.1 mg/ml) (*4*). The suspension was sonicated briefly (three 20-s bursts) during incubation. The lysate was centrifuged (4°C) at 150,000*g* for 30 min, and the supernatant was recovered.
14. M. Vaara, *Microbiol. Rev.* **56**, 395 (1992).
15. K. B. Seamon, J. W. Daly, H. Metzger, N. J. DeSouza, J. Reden, *J. Med. Chem.* **26**, 436 (1983).
16. E. M. Sutkowski, W.-J. Tang, C. W. Broome, J. D. Robbins, K. B. Seamon, *Biochemistry* **33**, 12852 (1994).
17. K. B. Seamon and J. W. Daly, *Adv. Cyclic Nucleotide Res.* **20**, 1 (1986).
18. A. Kashiwagi, T. P. Heucksteadt, J. E. Foley, *J. Biol. Chem.* **258**, 13685 (1983).
19. H. G. Joost, A. D. Habberfield, I. A. Simpson, A. Laurenza, K. B. Seamon, *Mol. Pharmacol.* **33**, 449 (1988).
20. T. Hoshi, S. S. Garber, R. W. Aldrich, *Science* **240**, 1652 (1988).
21. P. K. Wagoner and B. S. Pallotta, *ibid.*, p. 1655.
22. G. Heuschneider and R. D. Schwartz, *Proc. Natl. Acad. Sci. U.S.A.* **86**, 2938 (1989).
23. S. Wadler and P. H. Wiernik, *Cancer Res.* **48**, 539 (1988).
24. D. I. Morris, L. A. Speicher, A. E. Ruoho, K. D. Tew, K. B. Seamon, *Biochemistry* **30**, 8371 (1991).
25. B. E. Wadzinski, M. F. Shanahan, K. B. Seamon, A. E. Ruoho, *Biochem. J.* **272**, 151 (1990).
26. D. I. Morris *et al.*, *Mol. Pharmacol.* **46**, 329 (1994).
27. R. A. Johnson and I. Shoshani, *J. Biol. Chem.* **265**, 11595 (1990).
28. V. A. Florio and E. M. Ross, *Mol. Pharmacol.* **24**, 195 (1983).
29. The 60-kD protein has recently been purified to near homogeneity; these preparations are devoid of other immunoreactive bands. It is thus clear that the 60-kD protein is the active species. The turnover number of the purified protein is similar to the value for purified type II adenylyl cyclase (C. Dessauer and A. G. Gilman, unpublished data).
30. Supernatants (60 μg) were alkylated with *N*-ethylmaleimide, resolved by SDS–polyacrylamide gel electrophoresis (11% gels), transferred to nitrocellulose, and stained with affinity-purified antiserum C2-1077 directed against the COOH-terminus of type II adenylyl cyclase.
31. The soluble fraction (200 μl) from *E. coli* expressing IC_1IIC_2-L_3 was applied to a Pharmacia Superdex 75 HR 10/30 gel-filtration column that had been equilibrated with 20 mM tris-HCl (pH 8.0), 1 mM EDTA, 2 mM dithiothreitol, and 500 mM NaCl. The flow rate was 0.3 ml/min, and 0.3-ml fractions were collected. Adenylyl cyclase activity was measured in the presence of 10 mM $MgCl_2$ and 100 μM forskolin. Portions of selected fractions were subjected to SDS–polyacrylamide gel electrophoresis and immunoblot analysis.

32. We thank M. Stanzel for technical assistance, C. Dessauer for correcting the sequence of pTrc-IC_1IIC_2-L_3, A. Danchin for *E. coli* Δcya strains TP2000 and TP2339, J. I. Gordon for plasmid pBB131, C. Berlot for mutants of $G_s\alpha$, and A. Beuve and W. Epstein for helpful discussions. Supported by American Heart Association grant 92G-078 (to W.-J.T.) and by NIH grant GM34497, American Cancer Society grant BE30-O, the Lucille P. Markey Charitable Trust, and the Raymond and Ellen Willie Chair of Molecular Neuropharmacology.

6 January 1995; accepted 3 April 1995

Common Mechanisms of Visual Imagery and Perception

Alumit Ishai* and Dov Sagi

Detection of a visual target can be facilitated by flanking visual masks. A similar enhancement in detection thresholds was obtained when observers imagined the previously perceived masks. Imagery-induced facilitation was detected for as long as 5 minutes after observation of the masks by the targeted eye. These results indicated the existence of a low-level (monocular) memory that stores the sensory trace for several minutes and enables reactivation of early representations by higher processes. This memory, with its iconic nature, may subserve the interface between mental images and percepts.

Visual imagery is the invention or recreation of a perceptual experience in the absence of retinal input. Brain imaging studies implicate activity in cortical visual areas during visual imagery (*1*, *2*), yet the neural mechanisms that subserve "seeing with the mind's eye" are controversial (*3*, *4*). The degree to which the same neural representations are involved in both visual imagery and visual perception is unclear. Earlier studies have shown that visual imagery interferes with perception (Perky effect) (*5*). Visual imagery can facilitate letter detection by increasing expectation (*6*), yet there is no evidence for direct facilitatory interactions between imagery and perception. In order to test whether visual imagery can induce a facilitatory effect on visual perception, we used a lateral masking detection paradigm (*7*, *8*), in which human observers

Department of Neurobiology, Brain Research, Weizmann Institute of Science, Rehovot 76100, Israel.

*To whom correspondence should be addressed.